

An Experimental Study of Accelerating Phase Change Heat Transfer

Yool-Kwon Oh*, Seul-Hyun Park

School of Mechanical Engineering., Chosun University, Gwangju 501-759, Korea

Kyung-Ok Cha

School of Mechanical Engineering., Myongji University, Seoul 120-728, Korea

The present paper investigated the effect of ultrasonic vibrations on the melting process of a phase-change material (PCM). Furthermore, the present study considered constant heat flux boundary conditions unlike many of the previous researches adopted constant wall temperature conditions. Therefore, in the present study, modified dimensionless parameters such as Ste^* and Ra^* were used. Also, general relationships between melting with ultrasonic vibrations and melting without ultrasonic vibrations were established during the melting of PCM. Experimental observations show that the effect of ultrasonic vibrations on heat transfer is very important throughout the melting process. The results of the present study reveal that ultrasonic vibrations accompany the effects like agitation, acoustic streaming, cavitation, and oscillating fluid motion. Such effects are a prime mechanism in the overall melting process when ultrasonic vibrations are applied. They enhance the melting process as much as 2.5 times, compared with the result of natural melting. Also, energy can be saved by applying ultrasonic vibrations to the natural melting. In addition, various time-wise dimensionless numbers provide conclusive evidence of the important role of ultrasonic vibrations on the melting phenomena.

Key Words : Ultrasonic Vibrations, PCM, Phase Change Heat Transfer, Acoustic Streaming, Cavitation, PIV

Nomenclature

h : Heat transfer coefficient
 Δh_f : Latent of fusion
 g : Gravitational acceleration
 t : Time
 q'' : Heat flux
 C_p : Specific heat of liquid phase
 H : Height of solid paraffin (Characteristic Height)
 K : Thermal conductivity of liquid phase
 T : Temperature
 F_o : Fourier number
 Nu : Nusselt number

Pr : Prandtl number
 Ra : Rayleigh number
 Ra^* : Modified Rayleigh number
 Ste : Stefan number
 Ste^* : Modified Stefan number

Greeks

α : Thermal diffusivity of liquid phase
 β : Thermal expansion coefficient
 θ : Dimensionless Temperature
 ν : Kinematic viscosity

Subscript

f : Fusion
 h : Heater surface
 i : Solid-liquid interface
 l : Liquid
 s : Solid

* Corresponding Author,

E-mail : ygoh@mail.chosun.ac.kr

TEL : +82-62-230-7014; FAX : +82-62-232-9218

School of Mechanical Engineering, Chosun University, Gwangju 501-759, Korea. (Manuscript Received August 29, 2001; Revised October 15, 2001)

1. Introduction

Solid-liquid phase change (i. e. melting or solidification) occurs in a number of situations of practical interest. Some common examples include the melting of edible oil, metallurgical process such as casting and welding, and materials science applications such as crystal growth. Therefore, due to the practical importance of the subject, there have been a large number of experimental and numerical studies of problems involving phase change. Numerous researches involving phase change problem have been conducted since Cho and Sunderland (1969) observed the melting phenomena. Chan et al. (1983) developed the theory of melting phenomena based on two-phase region, i. e. solid and liquid regions. Gau and Viskanta (1986) measured the melting speed and heat transfer coefficient of a pure metal (Gallium) and obtained a heat transfer correlation in terms of dimensionless parameters such as Ra, Ste, and Nu number. However, most researches (Cho and Sunderland, 1969; Chan et al., 1983; Gau and Viskanta, 1986) focused on conduction or natural convection heat transfer. Only a few papers (Lemlich, 1955; Larson and London, 1962; Topp and Eisenklan, 1972; Fsairbanks, 1979; West and Taylor, 1952) dealt with the effect of ultrasonic vibrations during the melting process. Even though Hong (1988) suggested that ultrasonic vibrations increased the melting rate, its applications have been restricted to the chemical and medical industries.

The objective of the present study was to investigate the melting process of a PCM from a heated vertical wall for the following : one without ultrasonic vibrations (natural melting) and the other with ultrasonic vibrations. Furthermore, the present study considered constant heat flux boundary conditions unlike many of the previous researches which had adopted constant wall temperature conditions. Paraffin was selected as the PCM since its thermophysical properties (Lee and Uan, 1999) were well-known. It is much less expensive and more easily available than

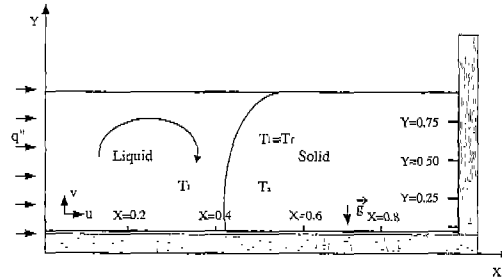


Fig. 1 Two dimensional model for melting procedure

Hexadecane or Tetradecane. Moreover, paraffin is more stable in phase-change region, and excellent for the phase-change heat transfer study.

2. Model for Melting Process

Hong (1988) and Ho and Viskanta (1986) developed a theoretical analysis based on their two-dimensional model. They presented modified dimensionless parameters such as Ra and Ste, respectively. In the present study, their model and fundamental equations were partially adopted. Figure 1 presents a two-dimensional model for the melting problem. In the present study, the wall temperature increased until the melting was completed because a constant heat flux boundary condition was considered. Hence, modified Stefan and Rayleigh numbers were used instead of Stefan and Rayleigh numbers as follows :

$$Ste = \frac{C_p \Delta T}{\Delta h_f} \tag{1}$$

$$Ra = \frac{g \beta \Delta T H^3 Pr}{\nu^2} \tag{2}$$

Where, $\Delta T = \frac{q'' H}{K}$

$$Ste^* = \frac{C_p q'' H}{K \Delta h_f} \tag{3}$$

$$Ra^* = \frac{g \beta q'' H^4 Pr}{K \nu^2} \tag{4}$$

The natural convection in the liquid region can be considered to be quasi-steady state because the solid-liquid interface moves slowly. Experimental evidence (Gadgil and Gobin, 1984) indicates that the flow remains entirely laminar in the range of

Ra numbers, $10^6 < Ra < 10^9$. Note that the transition to turbulence occurs at Ra numbers greater than 109. As Okada (1984) and Sparrow et al. (1977) reported, Prandtl number does not affect the melting rate for $Pr > 7$ when Rayleigh number is used. In the present study, only a single value of Prandtl number ($Pr=40$) was used. Modified Rayleigh numbers depending on heat flux were constant ($Ra^* = 5.80 \times 10^7$, $Ra^* = 3.24 \times 10^7$) during the overall melting process.

3. Experimental Set-up and Procedure

3.1 Experimental set-up

Paraffin (n-octadecane) with the melting point of 52.3°C was selected as the PCM, and its properties are listed in Table 1. The test section consists of a tank and melting cavity as shown in Fig. 2. The melting cavity filled with paraffin is positioned inside the tank which is filled with water. The water in the tank was used in order to protect ultrasonic vibrators from electric overload when ultrasonic vibrations are applied to the solid paraffin in the beginning of melting. Also, it can minimize heat conduction to the solid paraffin from vibrators when vibrators are heated. The melting cavity has an inner dimension of 13 cm height, 12.5 cm length, and 12.5 cm width.

A stainless steel plate heater vertically positioned on one side of the cavity was heated, providing a constant heat flux regulated by an Automatic Voltage Regulator (AVR) during the overall melting process. The back of the heater surface was insulated with a bakelite plate and fiberglass so that the heat flux would propagate only to the forward direction from the heater surface. In addition, all four outside walls of the cavity were covered with styrofoam and fiberglass plate. The frequency generator was monitored by an oscilloscope.

Eight chromel–alumel thermocouples (K type) were installed at pre-selected locations ($X=0.2, 0.4, 0.6,$ and 0.8 , see Fig. 1) in the melting cavity to measure the temperature distribution during the melting process. Each thermocouple was wound in insulation tape and sheathed in a

Table 1 Thermophysical properties of paraffin

Properties	Value
Melting Temperature	52.3°C
Thermal Conductivity	$0.18 \text{ kcal/hr}^\circ\text{Cm}$
Density	863.03 kg/m^3
Specific Heat	$686.54 \text{ kcal/kg}^\circ\text{C}$
Viscosity	$1.00 \text{ m}^2/\text{hr}$
Heat of Fusion	57.74 kcal/kg
Thermal Expansion Coefficient	0.001

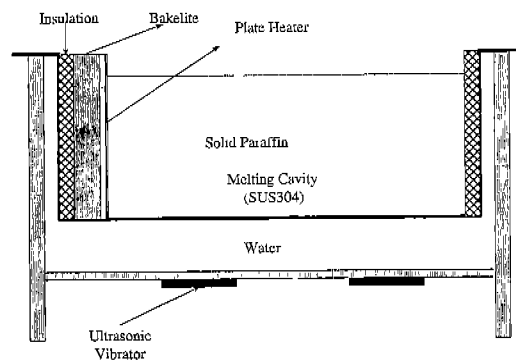


Fig. 2 Schematic diagram of test section

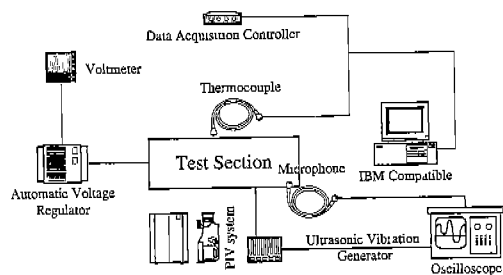


Fig. 3 Schematic diagram for experimental set-up

stainless steel tube to minimize heat conduction. All thermocouples were connected to a data acquisition controller. The temperatures at different positions were automatically recorded at a PC for data record. Figure 3 shows a schematic diagram for the present experimental set-up. As shown in the Fig. 3, Particle Image Velocimetry (PIV) was also adopted for visualization and a self-made microphone was used to measure the pressure distributions in the liquid region when ultrasonic vibrations were applied.

3.2 Experimental procedure

Solid paraffin was first melted, and thus the melting cavity was filled up with melted paraffin. Before experiments were carried out, the liquid paraffin was re-solidified in the melting cavity. After solidification, some liquid paraffin was also supplied to fill up depressed spots caused by the contraction of the paraffin during the solidification process. Slight irregularities and grooves on the top surface of the paraffin were removed by melting them with hot air. The temperature of the paraffin was initially maintained at room temperature (26°C) before each test was performed. To keep the whole solid paraffin at room temperature, it was left at room temperature for one day. After the solid temperature equilibrium was obtained, a constant heat flux condition was applied. In order to obtain accurate data, tests were repeated twice at two different heat fluxes :

- (1) $q'' = 9905.1 \text{ kcal/hrm}^2$ ($Ra^* = 5.80 \times 10^7$)
- (2) $q'' = 5535.2 \text{ kcal/hrm}^2$ ($Ra^* = 3.24 \times 10^7$)

Once an experiment began, the heater temperature was measured every one minute during the total melting process. Generally, the physical properties of the paraffin changed above 200°C because the continuous chains of each carbon atom were apt to break up at that temperature. (Hong, 1990) Hence, two different heat fluxes are considered. Heater surface temperature was kept below 200 °C at these heat flux levels. To obtain a constant heat flux boundary condition, a plate heater was heated electrically by an automatic voltage regulator (Powertek, PAV-500) which was designed to maintain the constant output voltage within $\pm 1\%$ of nominal, with an input voltage variation of $\pm 20\%$. Prior to the experiments, all thermocouples were calibrated with a calibration voltage source. The melting was carried out three times under the same condition in order to the accurate temperature distribution for each experimental case. The largest temperature deviation on the heater surface was about $\pm 5\text{ }^\circ\text{C}$, compared to the average temperature. However, in the case of temperature in PCM, the largest deviation was about $\pm 2\text{ }^\circ\text{C}$. In the

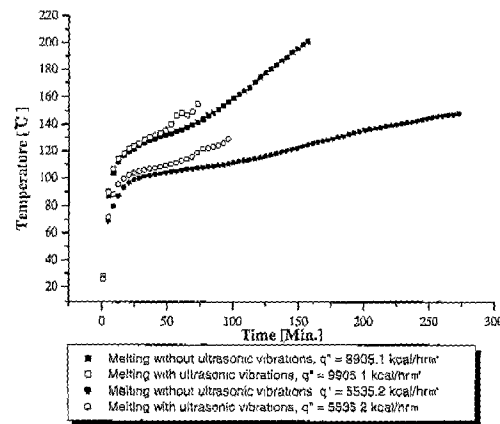


Fig. 4 Average temperature distribution on a heater surface

present study, a fixed frequency level of 40 kHz was selected, but power levels were varied from 70 to 340 W in order to investigate the effect of the strength of ultrasonic vibrations on the phase-change heat transfer.

4. Heat Transfer on the Heater Surface and in the Liquid

4.1 Temperature distributions on the heater surface

Figure 4 shows average temperature distributions on a heater surface under two experimental conditions : melting without ultrasonic vibrations and melting with ultrasonic vibrations. Heater temperature was increased for the first 15 minutes because the conduction heat transfer from the heater surface to the PCM was predominant regardless of heat flux and melting condition. Temperature started to increase slowly when natural convection mode was activated. In the case of melting with ultrasonic vibrations, sudden temperature increase on the heater surface was observed near the end of melting, which can be attributed to the fact that the heater surface was heated due to some dried areas when bubbles formed by ultrasonic vibrations slipped along the heater surface.

The melting time was shortened as much as about 2.5 times because of cavitation, acoustic streaming and thermal oscillation [1].

compared with that of the natural melting case. Actually, most of melting was completed after sudden temperature increases on the heater surface. It means that accelerating factors of melting such as cavitation, acoustic streaming and thermal oscillating flow motion are activated after sudden temperature increases on the heater surface. Details will be discussed next.

4.2 Heat transfer coefficient on the heater surface

In the early stage of melting, conduction dominated the heat transfer in the melt region, judging from the fact that the molten region appeared to be uniformly parallel to the vertical heater. As the heating continued, the buoyancy-driven convection in the melt started to develop and continued to intensify as evidenced by the appearance of a nonuniform melting front receding from the free surface to the bottom.

As aforementioned, the melt reached the maximum temperature near the free surface and then moved downward along the solid-liquid interface, losing heat and contributing its energy to the melting of the solid paraffin. Therefore, its ability to melt the solid paraffin gradually decreased to the minimum at the bottom of the cavity. The onset of convection may improve the overall heat transfer rate. If both heat transfer modes are considered simultaneously, the heat transfer coefficient can be written as Nusselt number on the heater surface as follows :

$$Nu = \frac{q'' H}{\Delta T K} \quad (5)$$

Where, ΔT is the difference between heater temperature and temperature of fusion of PCM. The correlation between the Nusselt number and $F_o Ste^*$ is depicted in Fig. 5 for different heat fluxes and two experimental conditions, where, the Nusselt number divided by $Ra^{*0.25}$ is plotted as a function of dimensionless parameter $F_o Ste^*$. Where, Fourier number, F_o is a dimensionless time parameter which represents the ratio of heat transfer by conduction to the energy-storage rate within the material. It is normally defined in the following forms:

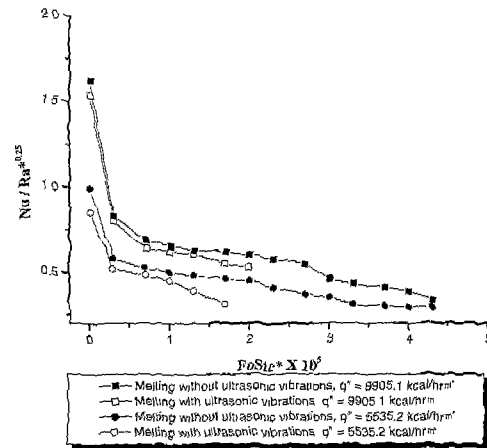


Fig. 5 Nusselt number variation on a heater surface with respect to $F_o Ste^*$

$$F_o = \frac{\alpha \cdot t}{H^2} \quad (6)$$

Fourier number multiplied by modified Stefan number, Ste^* which means the ratio of sensible heat to latent heat during melting. Consequently, $F_o Ste^*$ can be used as a dimensionless parameter to present the solid-liquid heat transfer problem. Other investigators (Gau and Viskanta, 1986; Ho and Viskanta, 1986) also used these dimensionless parameters. The power of 0.25 over Ra^* was generally used in the natural convection.

As shown in Fig. 5, the Nusselt number was very high in the beginning of the melting process, and decreased drastically until $F_o Ste^*$ reached approximately 0.3×10^5 , which is slightly depending on Ra^* and then it decrease slowly. These results lead to a significant conclusion that conduction mode is dominant during the early stage of melting of PCM (i. e., $0 < F_o Ste^* < 0.3 \times 10^5$). After this point ($F_o Ste^* = 0.3 \times 10^5$), it decreased slowly as the melt zone became wider. The difference in the Nusselt number for each heat flux case came from the Rayleigh number which greatly depended upon the heat flux. That is, the higher the Rayleigh number is, the more active the convection is. Thus one can conclude that the melting process can be described as a function of F_o , Ste^* , and Ra^* as shown in Fig. 5. For the case with ultrasonic vibration, the heat transfer coefficient on the heater surface was fur-

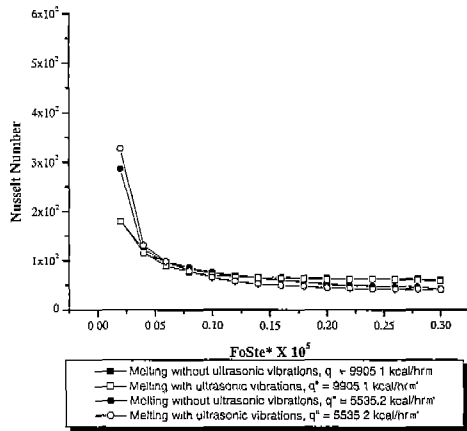


Fig. 6 Nusselt number variation on the heater surface during conduction with $FoSte^*$

ther affected by ultrasonic vibrations decreasing slightly faster than the case without the ultrasonic vibration after $FoSte^*$ reached approximately $1.0-1.3 \times 10^5$. Such points (i. e., $FoSte^* = 1.0-1.3 \times 10^5$) are in good agreement with the points from which heater surface temperature starts suddenly as given in Fig. 4. Also, most of the solid paraffin began to melt after this point when ultrasonic vibrations were applied. Hence, one can conclude that there are extra effects such as cavitation, acoustic streaming, thermal oscillating flow and strong agitation to enhance the melting rate by ultrasonic vibrations in this period.

In order to examine the effect of the conduction heat transfer on the melting process of the PCM, the effect of Rayleigh number was excluded, and the Nusselt number is plotted in a range of $0 < FoSte^* < 0.3 \times 10^5$, in Fig. 6. Nusselt numbers on the heater surface were almost the same in the beginning of melting for two different experimental conditions when the Rayleigh number was excluded. Ultrasonic vibrations activate some fluid dynamics phenomena. One of the fluid dynamics phenomena, bubbles can affect the heat transfer coefficient on the heat surface, as aforementioned. That is, the heat transfer coefficient on the heater surface decreased slightly than the case without the ultrasonic vibration especially after $FoSte^*$ reached approximately $1.0-1.3 \times 10^5$ as shown in Fig. 5. However, during

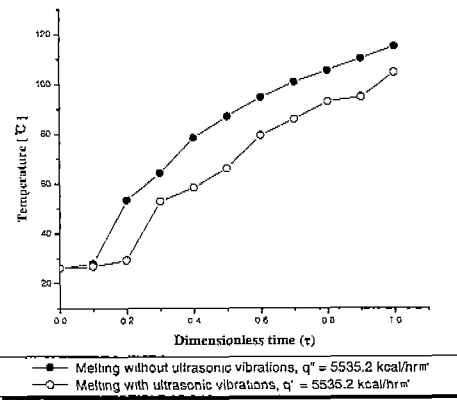


Fig. 7 Temperature distribution at $X=0.2$ and $Y=0.5$ with dimensionless time (τ)

conduction mode, the heat transfer coefficients on the heat surface were almost same under different experimental conditions because such fluid dynamics phenomenon was not activated in spite of applying ultrasonic vibrations in this period.

Consequently, one can conclude that ultrasonic vibrations did not make much impact on the conduction mode. Ultrasonic vibrations did not increase the heat transfer coefficient on the heater surface but accelerated the melting rate of the PCM.

4.3 Augmentation of heat transfer in the liquid

Ultrasonic vibrations greatly affect the melting rate, but does not improve the heat transfer coefficient on the heater surface. It is because the governing factor of heat transfer coefficient on the heater surface is heater surface temperature, which can be affected by cavitation and bubbles near the end of melting. Therefore, it is necessary to investigate temperature distribution of PCM in order to find what accelerates melting rate.

Figure 7 shows the temperature history of PCM at $X=0.2$ and $Y=0.5$ against normalized time, τ , for two different experimental conditions. The normalized time was obtained by dividing time by the total time consumed to melt the PCM completely. The temperature of the PCM was lower by $15-20^\circ\text{C}$ for the case of ultrasonic vibrations than the case without ultrasonic vibrations. The

temperature history of the PCM at other locations also showed the similar trends. In short, ultrasonic vibrations increased the heat transfer coefficient in the liquid. Factors to enhance heat transfer coefficient in the liquid by ultrasonic vibrations are discussed next:

4.3.1 Acoustic streaming

Applying ultrasound in a medium may cause the flow velocity of the medium to increase ; an effect known as acoustic streaming (Barnett, 1998 ; Affel and willert, 1998) In the present study, applying ultrasonic vibrations to the liquid were found to induce acoustic streaming, which was clearly observed from the velocity field measured by PIV. Actually, acoustic streaming results from the attenuation of the acoustic wave in the liquid. Acoustic streaming has been shown to enhance both thermal convective streaming and mass transport, where convective transport is superimposed on diffusive transport. (Folger and Loud, 1973) A typical map of the induced upward flow (acoustic streaming) appears in Fig. 8. Strong acoustic streaming with mean velocity, 3.6 cm/s was well developed near two ultrasonic transducers.

4.3.2 Cavitation

Cavitation is a result of acoustic waves introduced into the liquid by means of a series of transducers mounted to the test enclosure. In the compression wave, the molecules of the liquid are compressed together tightly. Conversely, in the expansion wave, the molecules are pulled apart rapidly. The expansion is so dramatic that the molecules are ripped apart, creating microscopic bubbles. The bubbles contain a partial vacuum while they exist. As the pressure around the bubbles becomes greater, the fluid around the bubble rushes in, collapsing the bubble very rapidly. When this occurs, induced flow (acoustic streaming) is created that may travel at this very high rate. The acoustic pressure amplitude was acquired by self-made microphone for the liquid. (Fig. 9) The precise measurement of acoustic pressure was not done, but the maximum acoustic pressure amplitude is approximately 1×10^5 Pa.

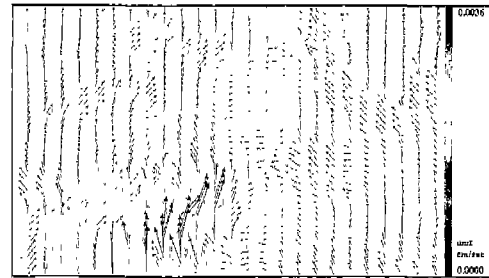


Fig. 8 Two dimensional velocity field of induced acoustic streaming by ultrasonic vibrations

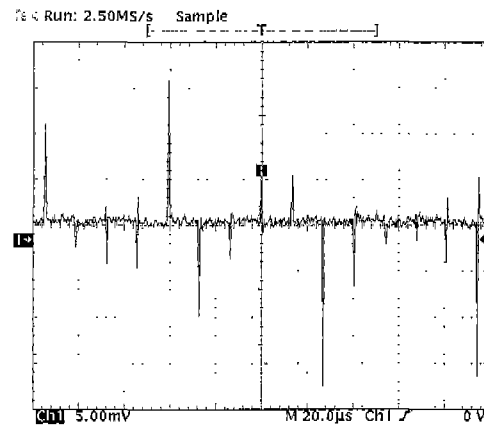


Fig. 9 Waveform of acoustic pressure amplitude at $20 \mu\text{s}/\text{division}$

(Takaaki et al., 2001) In order to investigate the frequency of acoustic pressure, the horizontal scale (time per division) was changed from $20 \mu\text{s}$ to $5 \mu\text{s}$. (Fig. 10) As shown in Fig. 11, the frequency of amplitude of acoustic pressure is about 77kHz. One amplitude of acoustic pressure is also enlarged in Fig. 10 by reducing the horizontal scale to 250 ns. Some pressure fluctuations are observed in an amplitude of acoustic pressure. Such fluctuations formed by the collapse of cavitation and acoustic streaming seem to develop the thermal oscillating flow.

4.3.3 Thermal oscillating flow

Acoustic streaming with cavitation can generate thermal convective streaming and it accelerates the melting process. And then this thermal convective flow developed into a severe fluid motion. It is a gross movement of the fluid

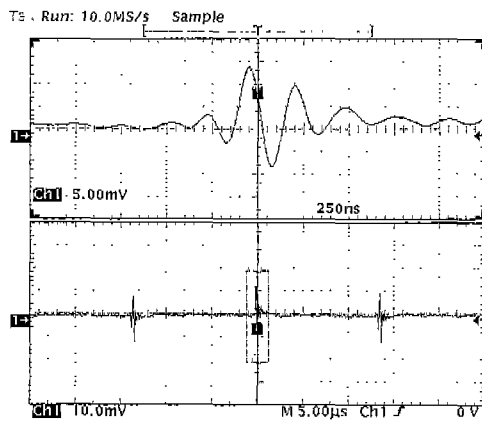
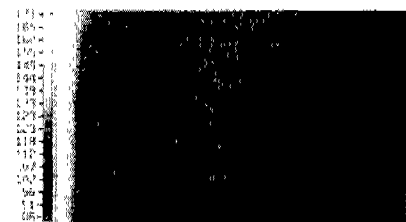
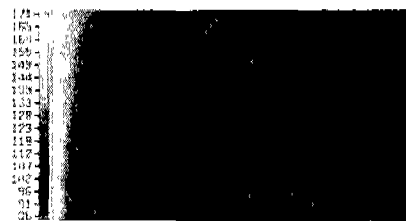


Fig. 10 Acoustic pressure amplitude at $5\mu\text{s}/\text{division}$ (below) and enlarged pressure amplitude (above)



(a) Melting without ultrasonic vibrations



(b) Melting with ultrasonic vibrations

Fig. 11 Development of thermal oscillating flow by ultrasonic vibrations

in the liquid. This force, acoustic streaming, and cavitation effect seem to increase the melting speed. Figure 11 shows the thermal oscillating flow captured by infrared thermal camera when ultrasonic vibrations are applied to the liquid. As the hot liquid moves upward along the heater surface, it gains energy and reaches the highest temperature near the free surface. After reaching the maximum temperature, the liquid makes a turn, deflecting away from the heater surface to the solid paraffin. Therefore, temperature distributions are more stable in the natural

melting case (Fig. 12(a)). However, Fig. 12(b) shows ultrasonic vibrations made strong thermal convective flow. Thermal convective flow is closely connected with agitation effect and acoustic streaming. Thermal convective flow become intensified as the effects of acoustic streaming increase. Actually Ha (1992) mentioned oscillating flow should be developed in a high intensity acoustic field.

As aforementioned, the melting speed was 2.5 times faster than that without ultrasonic vibrations when ultrasonic vibrations were applied. Hong (1988) reported that the frequency of up to 55 kHz can reduce the melting time and that there was no further improvement of melting speed beyond that frequency. However, most ultrasonic devices like ultrasonic cleaners and ultrasonic humidifiers have adopted the output power variation instead of frequency variation because it is not easy to vary the frequency with one frequency generator. So the output power level at a frequency generator was adjusted to investigate the effect of ultrasonic vibrations on melting phenomena in the present study. Table 2 shows the melting times when the output power levels were varied from 70 W to 340 W. at the frequency level of 40 kHz. The higher the output power level was, the faster the melting speed was. The total consumed electricity was also investigated for the following cases. ; melting with a heater and melting with a heater and ultrasonic vibrations. Table 3 shows that the melting time and the total consumed electricity at the same time in the case of melting with a heater and ultrasonic vibrations. However, in the present study, ultrasonic vibrations were transmitted through water as shown in Fig. 2. Therefore, the energy savings were not larger than expected. Table 3 shows energy consumption for the case of ultrasonic vibrations during the melting process. Clearly, energy can be saved by using ultrasonic vibrations. Energy consumption can be further minimized by adjusting the period of applying ultrasonic vibrations, considering that ultrasonic vibrations do not affect the conduction mode heat transfer.

Table 2 Melting time under variable output power level at a vibration generator

Heat Flux (kcal/hrm ²)	Output Power Level* (W)	Melting Time (Min.)
5535.2	70	164
5535.2	185	94
5535.2	340	72

* Output power level at ultrasonic vibration generator

Table 3 Comparison of total consumed electricity for the overall melting process

Total consumed electricity (Wh)	Heater	Vibrator	Melting time (Min.)
448.1*	448.1	-	161
445.9*	211.5	234.4	76
444.6*	444.6	-	275
441.8*	152.0	289.8	94

* Melting with a heater

+ Melting with a heater and ultrasonic vibrations

6. Conclusions

The melting process in the melting cavity with a heated vertical wall has been studied under two experimental conditions. : (1) Natural melting and (2) Natural melting with ultrasonic vibrations. The present study focused on observing the general phenomena and explained why such phenomena occurred for each experimental condition rather than focusing on each phenomena itself. The melting process with ultrasonic vibrations is 2.5 times as fast as the natural melting due to cavitation, acoustic streaming, and thermal oscillating flow. Also, energy can be saved by applying ultrasonic vibrations, compared to the natural melting. Energy consumption rate can be minimized by adjusting the period of applying ultrasonic vibrations.

Acknowledgement

This study was supported (in part) by research funds from Chosun University.

References

- Affel, C. E. and Willert, K. J., 1998, "Particle Image Velocitmetry," A Particle Guide, Springer.
- Barnett, S. B., 1998, *Ultrasound Med. Biol.* 2, supp 1, pp. 28~29.
- Chan, S. H., Cho, D. H. and Kocamustafaogullari G., 1983, "Melting and Solidification with Internal Radiative Transfer," *Int. J. Heat Mass Transfer*, Vol. 26, No 4, pp. 621~630.
- Cho, S. H. and Sunderland, J. E., 1969, "Heat conduction Problems with Melting or Freezing," *Journal of Heat Transfer*, pp. 125~131.
- Folger, S. and Loud, K., 1973, *J. Acous. Soc. Am.* 53, pp. 59.
- Fsairbanks, H. V., 1979, "Influence of Ultrasound upon Heat Transfer Systems," *Ultrasonics Symposium*, pp. 384~389.
- Gadgil, A. and Gobin D., 1984, "Analysis of Two-Dimensional Melting in Rectangular Enclosures in Presence of Convection," *Transaction of the ASME*, Vol. 106, pp. 20~26.
- Gau, C. and Viskanta, R., 1986, "Melting and Solidification of a Pure Metal on a Vertical Wall," *J. of Heat Transfer*, vol. 108, pp. 204~209.
- Ha, M. Y., 1992, "A Theoretical Study on the Acoustically Driven Oscillating Flow around Small Spherical Particales," *KSME Int. Journal*, Vol 6, No. 1, pp. 49~57.
- Ho, C. J. and Viskanta, R., 1986, "Heat -Transfer During Melting from the Isothermal Vertical Wall," *J. of Heat Transfer*, Vol. 108, pp. 204~209.
- Hong, J. S., 1988, "Experimental Study of Melting Phenomena with and without ultrasonic vibrations," M. S. Thesis, Univ. of Illinois at Chicago.
- Hong, C. S., 1990, "Studies on Heat Storing and Retrieving Characteristics in a Paraffin-Filled Horizontal Circular Tube," Ph. D. Thesis, Seoul National University.
- Larson, M. B. and London, A. L., 1962, "A Study of the Effect of Ultimate Vibrations on Convective Heat Transfer to Liquids," *ASME*, 62

-HT-44, pp. 62~68.

Lee, J. H., and Um, C. J., 1999, "An Experimental Study on the Ultrasonic Influence for Melting the Paraffin with Solid particles," *SACREK*, pp. 285~290.

Lemlich, R., 1955, "Effect of Vibration on Natural Convective Heat Transfer," *Industrial and Engineering Chemistry*, Vol. 47, No. 6, pp. 121~127.

Okada, M., 1984, "Analysis of heat transfer during melting from a vertical wall," *Int. J. Heat Mass Transfer*, Vol 27, No. 11, pp. 2057~2066.

Sparrow, E. M., Patankar, S. V. and Ramadhyani, S., 1977, "Analysis of Melting in

the Presence of Natural Convection in the Melt Region," *ASME Journal of Heat Transfer*, Vol. 99, No. 4, pp. 520~526.

Takaaki India, Xu Zhang and Akira Yabe, 2001, "Active Control of Phase Change from Supercooled Water to Ice by Ultrasonic Vibration 1," *Int. J. Heat and Mass Transfer* 44, pp. 4523~4531.

Topp, M. N. and Eisenklam, P., 1972, "Industrial and Medical Uses of Ultrasonic Atomizers," *Ultrasonics*, pp. 127~132.

West, F. B. and Taylor, A. T., 1952, "The Effect of Pulsations on Heat Transfer," *Chem. Eng. Progress.*, Vol. 48, No. 1, pp. 208~214.